NIH Public Access
Author Manuscript
Biochim Biophys Acta. Author manuscript; available in PMC 2011 February 1.

Published in final edited form as:
Biochim Biophys Acta. 2010 February ; 1803(2): 300–310. doi:10.1016/j.bbamcr.2009.11.002.

G Protein-Coupled Receptor Kinase 2 Activates Radixin, Regulating Membrane Protrusion and Motility in Epithelial Cells

Alem W. Kahsai[1], **Shoutian Zhu**[2], and **Gabriel Fenteany**[*]
Department of Chemistry, University of Connecticut, Storrs, CT 06269, USA

Abstract

Ezrin/radixin/moesin (ERM) proteins are membrane-cytoskeleton linkers that also have roles in signal transduction. Here we show that G protein-coupled receptor kinase 2 (GRK2) regulates membrane protrusion and cell migration during wound closure in Madin Darby canine kidney (MDCK) epithelial cell monolayers at least partly through activating phosphorylation of radixin on a conserved, regulatory C-terminal Thr residue. GRK2 phosphorylated radixin exclusively on Thr 564 *in vitro*. Expression of a phosphomimetic (Thr-564-to-Asp) mutant of radixin resulted in increased Rac1 activity, membrane protrusion and cell motility in MDCK cells, suggesting that radixin functions “upstream” of Rac1, presumably as a scaffolding protein. Phosphorylation of ERM proteins was highest during the most active phase of epithelial cell sheet migration over the course of wound closure. In view of these results, we explored the mode of action of quinocarmycin/quinocarcin analog DX-52-1, an inhibitor of cell migration and radixin function with considerable selectivity for radixin over the other ERM proteins, finding that its mechanism of inhibition of radixin does not appear to involve binding and antagonism at the site of regulatory phosphorylation.

1. Introduction

Cell migration is involved in a range of normal and disease processes, including embryonic development, immune function, tissue repair, angiogenesis and tumor metastasis. A common way to trigger cell migration is to mechanically perturb a cell monolayer through “scratch wounding.” In wounded Madin-Darby canine kidney (MDCK) epithelial cell monolayers, the cells move as a continuous unit with active protrusive force generation distributed from the wound edge to multiple rows of cells behind it in the moving cell sheet [1,2]. The migration of the MDCK cell sheet involves the Rho-family small GTPase Rac [1], phosphoinositides [1], c-Jun N-terminal kinase [3], Raf kinase inhibitor protein [4], ADP-ribosylation factor 6 [5,6] and glycogen synthase kinase 3 [6]. While wound closure depends on Rac activity, Rho and Cdc42, other members of the Rho GTPase family (for reviews, see refs. [7,8]), are not required in MDCK cell sheets for wound closure itself, but they do regulate how evenly the wound edge advances [1]. Closure of small wounds in MDCK cell monolayers is driven exclusively by cell migration and not cell proliferation [2].

*Corresponding author. Tel: +1 860 486 6645; fax: +1 860 486 2981, gabriel.fenteany@uconn.edu (G. Fenteany).
[1]Current address: Howard Hughes Medical Institute, Department of Medicine, Duke University Medical Center, Durham, NC 27710, USA.
[2]Current address: Department of Chemistry, The Scripps Research Institute, La Jolla, CA 92037, USA.

Publisher's Disclaimer: This is a PDF file of an unedited manuscript that has been accepted for publication. As a service to our customers we are providing this early version of the manuscript. The manuscript will undergo copyediting, typesetting, and review of the resulting proof before it is published in its final citable form. Please note that during the production process errors may be discovered which could affect the content, and all legal disclaimers that apply to the journal pertain.

NIH-PA Author Manuscript
NIH-PA Author Manuscript
NIH-PA Author Manuscript

NIH-PA Author Manuscript

NIH-PA Author Manuscript

NIH-PA Author Manuscript

A semisynthetic derivative of the natural product quinocarmycin (also known as quinocarcin), DX-52-1, inhibits cell migration during wound closure in MDCK cell monolayers with a half-maximal inhibitory concentration for inhibition of wound closure at 24 h post-wounding of 140 nM [9]. DX-52-1 inhibits the function of the membrane-cytoskeleton linker protein radixin [9]. Radixin is a member of the ezrin/radixin/moesin (ERM) protein family that binds actin and membrane-associated proteins; ERM proteins are important for formation of diverse actin-rich cell-surface structures and also function in cell signaling (for reviews, see refs. [10–15]). ERM proteins may also have roles in tumor metastasis [16–18]. DX-52-1 perturbs both C-terminal interactions of radixin with actin and N-terminal interactions of radixin with certain membrane proteins, such as the cell adhesion protein CD44, the cell-surface receptor for hyaluronic acid [9]. In addition, DX-52-1 also binds the multifunctional carbohydrate-binding protein galectin-3, outside of its carbohydrate-binding site, but with slower kinetics than it does radixin [19].

In the inactive state, ERM proteins exist in a closed, auto-inhibited conformation in which the N-terminal FERM (band 4.1 and ERM) domain and C-terminal domain bind one another in a head-to-tail manner, thereby preventing association with their respective binding partners [10–13]). Activation of ERM proteins requires binding of the FERM domain to phosphatidylinositol-4,5-bisphosphate (PIP_2) followed by phosphorylation of a regulatory C-terminal Thr residue (Thr 567 of ezrin, Thr 564 of radixin and Thr 558 of moesin). In the activated open state, ERM proteins bind actin filaments and the membrane via integral and peripheral membrane proteins, such as CD43, CD44 and ERM-binding phosphoprotein 50 (EBP-50; also known as Na^+/H^+ exchanger regulatory factor 1).

Several kinases have been reported to phosphorylate ERM proteins on their regulatory C-terminal Thr residues, including Rho-kinase [20–22], protein kinase Cα [23], protein kinase Cθ [24], myotonic dystrophy kinase-related Cdc42-binding kinase [25], Nck-interacting kinase [26] and G protein-coupled receptor (GPCR) kinase 2 (GRK2) [27]. GRK2, also known as β-adrenergic receptor kinase 1, has been shown to be involved in the regulation of fibroblast and epithelial cell migration [28]. Furthermore, phosphorylation of ezrin by GRK2 results in membrane ruffling in carcinoma cells [27].

In the present study, we provide evidence that GRK2 regulates membrane protrusion and collective migration of a cell sheet during wound closure in MDCK cell monolayers at least partly through phosphorylation of ERM proteins, in particular radixin, and eliminate a possible mechanism for DX-52-1 involving antagonistic binding to the site of phosphorylation by GRK2 on radixin.

2. Materials and Methods

2.1. Cell culture

MDCK cells were purchased from the American Type Culture Collection and were maintained in a growth medium consisting of minimum essential medium (MEM) from Invitrogen with 10% newborn calf serum (HyClone) and in Dulbecco's modified Eagle's medium supplemented with 10% fetal bovine serum (Cellgro), respectively. Cells were incubated in a tissue culture incubator at 37°C and 5% CO_2.

2.2 Antibodies

Goat anti-radixin antibody (sc-6408), mouse anti-hemaglutinnin (HA) antibody (sc-7392) and rabbit anti-GRK2 antibody (sc-562) were from Santa Cruz Biotechnology, as were horseradish peroxidase (HRP)-conjugated secondary antibodies. Rabbit anti-actin antibody (A2066) was from Sigma. Mouse anti-Rac1 antibody (610650) and mouse anti-Cdc42 antibody (610928)

NIH-PA Author Manuscript

NIH-PA Author Manuscript

NIH-PA Author Manuscript

were from BD Biosciences/BD Transduction Laboratories. Rabbit anti-phospho-ERM antibody (3141) was from Cell Signaling Technology.

2.3. Silencing of GRK2 expression

Four target DNA sequences corresponding to nucleotides 568-588, 964-984, 1295-1315 and 1665-1685 relative to the start codon of the canine GRK2 gene were chosen with the siRNA Target Finder tool from Ambion. Knockdown of GRK2 in MDCK cells was achieved with a previously described short hairpin RNA (shRNA) expression vector [6] transfected into cells with Lipofectamine (Invitrogen), according to the manufacturer's instructions. Stable transfectants were selected in 400 μg/ml hygromycin (A.G. Scientific). There is an enhanced green fluorescent protein (GFP) expression cassette in the shRNA expression vector [6]. This allowed us to isolate GFP-positive stable transfectants with a fluorescence-activated cell sorter. Efficient knockdown (~90%) of GRK2, based on Western blot analysis with anti-GRK2 antibody, was achieved with the shRNA corresponding to nucleotides 568-588 of canine GRK2. As a control, we used cells stably transfected with the shRNA corresponding to nucleotides 964-984 of GRK2, since we found no change in GRK2 protein levels by Western blot analysis in these cells. Detection for Western blot analysis in these and subsequent experiments was with a species-appropriate HRP-conjugated secondary antibody and chemiluminescence according to the reagent manufacturer's procedure (GE Healthcare).

2.4. Fusion constructs and site-directed mutagenesis

Cloning of full-length murine radixin in the pVL1392 vector and N-terminal (amino acid residues 1-318) and C-terminal (residues 319-583) domains of murine radixin as glutathione-*S*-transferase (GST) fusions in pGEX-2T have been described previously [9,29]. The GFP-fusion construct of chicken radixin in pEGFP-N1 and the HA-fusion construct of murine radixin in pMFG have also been previously described [9,30]. The GST-fusion construct of human ezrin in pGEX-2T [31] was provided by Christian Roy (Université de Montpellier, France). The GST-fusion construct of human moesin in pGEX-4T1 [32] was provided by Vijaya Ramesh (Massachusetts General Hospital). Constructs for bovine wild-type GRK2 and the GRK2-K220R mutant in pcDNA3 [33,34] were provided by Philip B. Wedegaertner (Thomas Jefferson University). The GST-fusion construct of the p21-binding domain (PBD), which binds activated Rac1 and Cdc42, derived from murine p21-activated kinase 3 (PAK3) and cloned into pGEX-KG [35] was provided by Richard A. Cerione (Cornell University).

Site-directed mutagenesis was carried out with Stratagene's QuikChange kit, following the manufacturer's instructions. The sense oligonucleotide primers (with mutation sites underlined) used for mutagenesis of murine radixin (fused to GST) were 5′-GCCGTGATAAGTACAAG<u>GCC</u>CTTCGGCAGATTCG-3′ for the T564A mutation, 5′-GGCCGTGATAAGTACAAG<u>GAC</u>CTTCGGCAGATTCGACA-3′ for the T564D mutation, 5′-CGGCAGATTCGACAAGGCAAT<u>GCG</u>AAGCAGCGC-3′ for the T573A mutation. The sense primer used for the T564D mutation of chicken radixin (fused to GFP) was 5′-AGGCCGTGGTAAGTACAAG<u>GAT</u>CTTCGACAAATCCGACAA-3′. Success of mutation was verified by DNA sequencing.

2.5. Preparation of cells expressing different forms of radixin or GRK2

MDCK cells stably expressing GFP alone, GFP fusions of chicken radixin or radixin-T564D or murine radixin-HA were prepared by Lipefectamine-mediated transfection, followed by selection in growth medium with 500 μg/ml G418 sulfate (Geneticin) from Invitrogen. Transgene expression was confirmed by fluorescence microscopy and Western blot analysis. For GFP-expressing and GFP-fusion-expressing cells, GFP-positive cells were isolated with a fluorescence-activated cell sorter, while for radixin-HA-expressing cells, the use of cloning disks and serial dilution allowed for isolation of single transfectants. Transient transfection of

NIH-PA Author Manuscript

NIH-PA Author Manuscript

NIH-PA Author Manuscript

GRK2 or GRK2-K220R into the radixin-HA-expressing cells was also accomplished with Lipofectamine.

2.6. Wound closure assay and quantitation of membrane protrusion

Early passages of MDCK cells thawed from frozen stock cultures were used in all experiments. Wound closure experiments were conducted essentially as previously described [36]. The cell sheets were wounded with a micropipet fitted with ultramicro tips, and digital images of the wounded areas were acquired at different times post-wounding. The images were imported into NIH ImageJ software (http://rsbweb.nih.gov/ij/) for analysis. The number of membrane protrusions around the wound edge were counted to determine lamellipodial density at the margin (number of lamellipodial membrane protrusions divided by wound-edge perimeter length) as previously described [3]. Cell viability was evaluated at the end of each experiment by both the Trypan blue dye exclusion assay and observation of cell morphology, noting any rounding up and detachment of cells.

2.7. Fluorescence microscopy

MDCK cells stably transfected with GFP alone or GFP-fusion proteins were plated on glass coverslips in 12-well tissue culture plates and grown to confluence. Following wounding and incubation for 6 h at 37°C and 5% CO_2, cells were fixed with 4% formaldehyde and permeabilized with 0.5% Triton X-100 in phosphate-buffered saline (PBS) for 15 min. Cells were stained for filamentous actin with 50 nM tetramethylrhodamine isothiocyanate-conjugated phalloidin (TRITC-phalloidin; Sigma). Finally, after washing three times with PBS, coverslips were mounted onto glass slides in Mowiol 4–88 (0.1 g/ml) mounting medium (EMD Biosciences) containing 15 mg/ml of the antifade agent 1,4-diazabicyclo[2.2.2]octane (Sigma). Images were captured on an inverted fluorescence microscope (Leica DMI 6000B), equipped with a Hamamatsu Orca AG cooled charge-coupled device camera and controlled by PerkinElmer/Improvision Volocity software.

2.8. Expression and purification of recombinant proteins\

Expression and purification of full-length radixin from Sf9 cells using the baculovirus expression system was accomplished as previously described [9]. Since bacterial expression yields functional full-length ERM proteins as well [9,20,31,32,37], we also used this system for expression. GST-fusion proteins of radixin mutants (T564A, T564D and T573A), radixin N-terminal fragment, radixin C-terminal fragment, ezrin, moesin and PAK3 PBD were expressed in *Escherichia coli* strain BL21(DE3). Single bacterial colonies were picked to seed cultures in 500 ml of Luria-Bertani medium. After growing the cultures overnight, isopropyl-D-thiogalactopyranoside was added to 0.2 mM, followed by incubation for 3 h. Cells were then collected by centrifugation (5000 × *g*, 10 min). Bacterial pellets were resuspended in 25-ml ice-cold PBS containing 2 mM ethylene diamine tetraacetic acid (EDTA), 1 mM dithiothreitol (DTT), 100μg/ml lysozyme, 0.5% Triton X-100 and protease inhibitors [1 μg/ml leupeptin, 1 μg/ml pepstatin A, 0.1 mM phenylmethysulfonyl fluoride (PMSF) and 0.1 mM benzamidine]. Homogenized lysates were centrifuged (15,000 × *g*, 30 min, 4°C), and the resulting supernatants were mixed with 5 ml of a 1:1 slurry of glutathione-agarose beads (Sigma) in PBS, then incubated on a rotating wheel for 2 h at 4°C. Proteolytic cleavage to release ERM proteins, fragments and point mutants from the GST moiety was achieved by incubation with bovine thrombin (Sigma) for 12 h at 4°C in PBS, pH 7.4. Elution of GST-PBD was performed with 50 mM Tris, pH 8.0, 150 mM NaCl, 2.5 mM $CaCl_2$, 1 mM DTT and 10 mM glutathione. Purity of the resulting recombinant proteins was determined by sodium dodecyl sulfate (SDS)–polyacrylamide gel electrophoresis and staining with Coomassie blue.

NIH-PA Author Manuscript

NIH-PA Author Manuscript

NIH-PA Author Manuscript

2.9. Pull-down assays

The amount of GTP-bound Rac1 and Cdc42 was determined by an affinity pull-down assay with immobilized GST-PBD fusion protein, as previously described [6,38]. Equal amounts of whole-cell lysates from MDCK cells stably expressing GFP, radixin-GFP or radixin-T564D-GFP were incubated in RIPA buffer (50 mM Tris, pH 7.4, 150 mM NaCl, 1 mM EDTA, 0.5% sodium deoxycholate, 1% Nonidet P-40, 0.1% SDS, 2 mM DTT, 1 μg/ml leupeptin, 1 μg/ml pepstatin A, 0.1 mM PMSF, 0.1 mM benzamidine and 100 μM sodium orthovanadate) with ~20 μg GST-PBD and 30 μl glutathione-agarose beads on a rotating wheel for 2 h at 4°C. Following three cycles of washing in the same buffer to remove unbound proteins, with centrifugation (5000 × *g*, 5 min) between each wash to collect the beads, bound proteins were eluted from the beads with 30 μl of 2× SDS sample buffer. After boiling, samples were subjected to SDS-polyacrylamide gel electrophoresis and Western blot analysis with anti-Rac1 or anti-Cdc42 antibody. The levels of total Rac1 or Cdc42 were also determined by Western blot analysis.

2.10. Kinase assays

Purified baculovirally expressed GRK2 protein was provided by Robert J. Lefkowitz (Duke University Medical Center). The kinase activity of GRK toward purified recombinant ERM proteins, radixin point mutants, radixin N-terminal fragment and radixin C-terminal fragement as substrates was determined in a standard *in vitro* kinase assay. The reactions were performed in kinase buffer (20 mM Tris, pH 7.5, 150 mM NaCl, 10 mM $MgCl_2$, 0.5 mM EDTA, 0.5 mM ethylene glycol tetraacetic acid, 2 mM DTT, 1 μg/ml leupeptin, 1 μg/ml pepstatin A, 0.1 mM PMSF, and 0.1 mM benzamidine) with 200 nM GRK2, each substrate (1 μM of the full-length proteins or 2 μM of the truncated proteins), 50 μM ATP and 2 μCi [γ-^{32}P]-ATP (PerkinElmer) in the presence or absence of 25 μM porcine brain L-α-phosphatidylinositol-4,5-bisphosphate (PIP_2; Avanti Polar Lipids) and/or 50 nM bovine brain G protein βγ subunits (EMD Biosciences) in a final volume of 50 μl for 60 min at 30°C. The reactions were terminated by adding 25 μl of 2× SDS sample buffer followed by boiling for 5 min. Protein samples were resolved by SDS-polyacrylamide gel electrophoresis, and phospho-protein bands were visualized with a Bio-Rad Personal Molecular Imager.

2.11. Phosphorylation of ERM proteins in MDCK cells

MDCK cells were seeded in growth medium in 100-mm diameter tissue culture-treated polystyrene dishes and grown to confluence; the medium was then replaced with serum-free MEM for 24 h. After adding fresh medium, the monolayers were multiply wounded with plastic pipet tips, with 30 wounds across each plate. At the indicated times after wounding, cells were washed three times with ice-cold PBS and then lysed with 350 μl per plate of 2× SDS sample buffer. The whole-cell lysates were boiled for 10 min and centrifuged (15 min, 15,000 × *g*) prior to SDS-polyacrylamide gel electrophoresis and Western blot analysis. Blots were probed with anti-phospho-ERM antibody, then stripped and reprobed with anti-radixin antibody. The same procedure was followed for the analysis of phospho-ERM levels in MDCK cells transiently transfected with different GRK2 constructs.

2.12. DX-52-1-binding assay

The assay for DX-52-1 binding was performed as described previously [9,19]. Purified recombinant full-length radixin and its mutants (T564A, T564D and T573A), as well as ezrin and moesin were all tested under identical conditions: 23 μM protein solution (in a buffer of 20 mM Tris, pH 7.4, 150 mM NaCl, 2 mM EDTA, 2 mM DTT, 0.5% Triton X-100, 1 μg/ml leupeptin, 1 μg/ml pepstatin A, 100 μM PMSF and 100 μM benzamidine) with 10 μM biotinylated DX-52-1 with or without 50× molar excess of free, non-biotinylated DX-52-1 added simultaneously. After incubation at 4°C for 4 h, an equal volume of 2× SDS sample

NIH-PA Author Manuscript

NIH-PA Author Manuscript

NIH-PA Author Manuscript

buffer was added to each sample, followed by SDS-polyacrylamide gel electrophoresis and transfer to a polyvinylidene fluoride membrane as in conventional Western blotting. Detection of biotinylated DX-52-1-labeled proteins was achieved with streptavidin-HRP (Sigma) and chemiluminescence.

3. Results and Discussion

3.1. GRK2 positively regulates cell sheet migration during wound closure

We investigated the effect of silencing of GRK2 expression by stable transfection of a GRK2-specific shRNA cloned into a previously described shRNA expression vector [6]. The shRNA consisted of a hairpin loop and the sequence corresponding to positions 568–588 relative to the start codon of the canine GRK2 gene. The efficiency of GRK2 knockdown in the stably transfected cells was ~90% by Western blot analysis (Figure 1). We found that the GRK2-knockdown cells migrated more slowly than control cells during wound closure (Figure 1). This result suggests a positive role for GRK2 in the regulation of cell sheet migration during wound closure in MDCK cell monolayers, consistent with the results reported by Penela *et al.* [28].

3.2. Expression of a phosphomimetic radixin mutant increases membrane protrusion and motility

Phosphorylation of Thr 564 on radixin inhibits the association of its N- and C-terminal domains and results in conformational unmasking of its actin and membrane protein-binding ability (for reviews, see refs. [10–13]). Mutation of Thr 564 to a negatively charged residue, Asp or Glu, has been shown to result in a constitutively active phosphomimetic protein [39,40]. To examine the functional significance of the phosphorylation state of Thr 564 of radixin on epithelial cell sheet migration during wound closure, we prepared a mammalian expression construct encoding GFP fused to a radixin Thr-564-to-Asp mutant (radixin-T564D). We transfected this construct into MDCK cells and selected for stable expression, confirmed by fluorescence microscopy and Western blot analysis (Figure 2A).

We examined the effect of expression of the phosphomimetic radixin-T564D-GFP construct on MDCK cell morphology and migration following wounding of confluent monolayers. Cells expressing radixin-T564D-GFP displayed markedly increased levels of membrane protrusion and an aberrant morphology compared to the control GFP-expressing cells (Figure 2B–D). While less pronounced, the level of protrusive activity was also higher relative to the radixin-GFP-expressing cells, as quantitated in Fig. 2D. The high protrusive activity in the radixin-T564D-GFP-expressing cells was suppressed by treatment with the radixin inhibitor DX-52-1 (Figure 2B). Wound closure by radixin-T564D-GFP-expressing cells was considerably faster than by control GFP-expressing cells and slightly faster than by radixin-GFP-expressing cells (Figure 2E). In addition, expression of radixin-T564D-GFP resulted in loss of sensitivity of cells to the antimigratory activity of the radixin inhibitor DX-52-1 (Figure 2E), as did expression of radixin-GFP (Figure 2E and ref. [9]). The results suggest that radixin-T564D-GFP can titrate free DX-52-1 and reduce its effectiveness, just as radixin-GFP does, and implies that Thr 564 is not the site of alkylation of radixin by DX-52-1, something explored further later in this study.

3.3. Rac1 activity but not Cdc42 activity is elevated in radixin-T564D-GFP-expressing cells

Since expression of constitutively active radixin mutant in MDCK cells caused pronounced membrane protrusions at the wound edge, the levels of activated (GTP-bound) Rac1 and Cdc42 were evaluated. A pull-down assay with a GST-PBD fusion [6,38], which specifically binds to the GTP-bound forms of these small GTPases, was performed with MDCK cell extracts prepared from cells expressing GFP alone, radixin-GFP or radixin-T564D-GFP. Both activated

NIH-PA Author Manuscript

NIH-PA Author Manuscript

NIH-PA Author Manuscript

and total protein levels were determined by Western blot analysis with anti-Rac1 and anti-Cdc42 antibodies. The level of activated Rac1 in the radixin-T564D-GFP-expressing cells was markedly elevated above the controls, whereas the level of activated Cdc42 was unchanged (Figure 3).

Although the mechanism is currently unknown, radixin appears to lie in a signaling pathway, presumably as a scaffolding protein, "upstream" of Rac1, a conjecture supported by other studies [41,42]. ERM proteins may function both by regulating and being regulated by Rho-family GTPases in a positive feedback loop (for reviews, see refs. [43,44]). The Rho GDP dissociation inhibitor directly associates with ERM proteins, resulting in activation of Rho proteins [45]. At the same time, Rho proteins regulate ERM proteins, such as by positively affecting the interaction of ERM proteins with CD44 [46,47]. CD44 itself interacts with the guanine nucleotide exchange factor Tiam1 and stimulates Rac1 signaling [48]. The results collectively suggest that ERM proteins directly and indirectly participate in localized signaling feedback loops near the plasma membrane that are involved in cell adhesion, actin dynamics and cell migration. Our data suggest another possible feature of this process, whereby ERM proteins and their membrane-bound binding partners like CD44 may cooperatively regulate Rac1 signaling.

3.4. GRK2 phosphorylates the C-terminal region of radixin

A number of kinases have been reported to mediate the phosphorylation of ERM proteins at their regulatory C-terminal Thr residues [21–27]. GRK2 has been shown to phosphorylate Thr 567 of ezrin and regulate membrane ruffling in carcinoma cells [27]. GRKs are best understood as kinases that phosphorylate agonist-occupied GPCRs, allowing for the binding of β-arrestins to GPCRs, which prevents further GPCR signaling and results in their desensitization to agonist (for reviews, see refs. [49–51]). However, GRK2 also regulates a range of other proteins, including synucleins [52], phosducin [53], ribosomal protein P2 [54], the inhibitory γ subunit of the type 6 retinal cyclic guanosine monophosphate phosphodiesterase [55], the β subunit of the epithelial Na^+ channel [56], tubulin [57–59] and ezrin [27]. The role of GRK2 in epithelial cell motility is likely to be related to its ability to regulate non-GPCR proteins relevant to cell migration such as tubulin or ezrin.

We investigated the phosphorylation of full-length radixin and N- and C-terminal radixin fragments by GRK2 in the presence or absence of PIP_2 and G protein βγ subunits. PIP_2 affects the conformation of ERM proteins, opening them to their active state in which they can interact with their binding partners [47,60–62]. In addition, PIP_2 separately activates GRK2 [63]. Gβγ subunits are also activators of GRK2 [64,65]. Purified recombinant GRK2 robustly phosphorylated recombinant full-length radixin even in the absence of any GRK2 activator *in vitro*, and we saw very slight-to-no enhancement in the presence of activators (Figure 4Aand B). Under these conditions, the recombinant GRK2 was therefore activated to a near maximal level. The C-terminal radixin fragment (amino acid residues 319–583) was also phosphorylated by GRK2, whereas the N-terminal radixin fragment (residues 1–318) was not phosphorylated.

3.5. Radixin is phosphorylated by GRK2 exclusively on Thr 564

Radixin has two Thr residues near its C-terminal end, Thr 564 and Thr 573. To definitively establish that Thr 564 is the regulatory Thr residue phosphorylated by GRK2, we performed site-directed mutagenesis. Three mutants were generated – radixin-T564A, radixin-T573A and the phosphomimetic radixin-T564D – and then expressed and purified. The phosphorylation of these radixin mutants, the N- and C-terminal radixin fragments, moesin and ezrin by GRK2 was assessed. Challenging recombinant GRK2 with radixin-T564A or radixin-T564D as substrates resulted in little or no phosphorylation (Figure 5A, lanes 2 and 4, respectively). The N-terminal fragment of radixin was not phosphorylated either (Figure 5A, lane 5). In contrast,

NIH-PA Author Manuscript

NIH-PA Author Manuscript

NIH-PA Author Manuscript

radixin-T573A, the C-terminal radixin fragment, ezrin and moesin were effective substrates for GRK2 (Figure 5A, lanes 3, 6, 7 and 8, respectively). The quantitated values from triplicate experiments are shown in Figure 5B. The results demonstrate that Thr 546 is the exclusive site of phosphorylation of radixin by GRK2.

3.6. Phosphorylation of ERM proteins increases during the most active migratory phase of wound closure

In order to understand the functional importance of GRK2-mediated phosphorylation of the regulatory Thr residue of ERM proteins, particularly radixin, we examined the changes in phosphorylation state of ERM proteins before and after wounding of confluent MDCK cell monolayers by Western blot analysis with an anti-phospho-ERM antibody (that only recognizes ERM proteins phosphorylated on their regulatory C-terminal Thr residues: Thr 567 for ezrin, Thr 564 for radixin and Thr 558 for moesin). As shown in Figure 6A and B, the level of phosphorylated ERM was low in the unwounded monolayer and just after wounding. However, phosphorylation began to increase by 15 minutes post-wounding. High levels of phosphorylated ERM proteins were observed 1 h, 3 h and 6 h after wounding, when MDCK cells extend membrane protrusions and actively migrate into the open area left by the wound.

3.7. GRK2-dependent phosphorylation of ERM proteins in MDCK cells

We asked whether GRK2 activity is sufficient to induce the phosphorylation of ERM proteins in MDCK cells. The role of GRK2 in the activation of ERM proteins was evaluated by transiently transfecting radixin-HA-expressing MDCK cells with empty vector as a control, wild-type GRK2, kinase-dead GRK2 (GRK2-K220R) or GRK2-specific shRNA. Whole-cell lysates were prepared and subjected to Western blot analysis to determine the levels of phosphorylated ERM proteins with the anti-phospho-ERM antibody. Even though GRK2 appears ubiquitously expressed in MDCK cells by immunofluorescent staining (data not shown), transient overexpression of GRK2 still resulted in an increase in levels of phosphorylated ERM proteins compared to the control cells transfected with empty vector (Figure 7A and B). In contrast, knockdown of GRK2 or expression of kinase-dead GRK2 resulted in decreased levels of phosphorylated ERM proteins. The total levels of radixin remained unaffected, as determined by reprobing the same blots with the anti-radixin antibody. The degree of ERM-protein phosphorylation was lowest in the GRK2-knockdown cells, although some phosphorylation was still observed, presumably as a result of the activity of other kinases that can phosphorylate the C-terminal regulatory Thr residues of ERM proteins, such as Rho-kinase [20–22], protein kinase Cα [23], protein kinase Cθ [24], myotonic dystrophy kinase-related Cdc42-binding kinase [25], Nck-interacting kinase [26].

3.8. Thr 564 and Thr 573 are not the sites of modification by DX-52-1 on radixin, and ezrin and moesin are also modified by DX-52-1, but much less intensely than radixin

We previously showed that DX-52-1 binds the C-terminal region of radixin in a saturable and specific manner, disrupting interactions with both actin and CD44 [9]. The interaction with actin and CD44 are mediated by the C-terminal and N-terminal regions of radixin, respectively (for reviews, see refs. [10–15]). The structural effects of DX-52-1 on radixin appear complex, involving both short-range steric or conformational changes and long-range conformational changes. A possibility is that DX-52-1 may act by alkylating one of the C-terminal Thr residues, particularly the GRK2-phosphorylated Thr 564 residue.

We therefore investigated the binding of biotinylated DX-52-1 to the two Thr-to-Ala radixin mutants (radixin-T564A and radixin-T573A), where the nucleophilic Thr residues are converted to non-nucleophilic Ala residues, which cannot be phosphorylated or modified by DX-52-1. Mutation of Thr 564 or Thr 573 on radixin to Ala did not affect binding of biotinylated DX-52-1 (Figure 8A), consistent with the results shown in Figure 2E, where expression of

NIH-PA Author Manuscript

NIH-PA Author Manuscript

NIH-PA Author Manuscript

radixin-T564D-GFP in cells led to decreased sensitivity to DX-52-1, as did radixin-GFP (Figure 2E and ref. [9]). The results suggest that whatever nucleophile on radixin is specifically modified by DX-52-1, it is not one of these two Thr residues. We also evaluated the effect of DX-52-1 on phosphorylation of radixin by GRK2. Only a slight decrease in the phosphorylation of radixin was observed at high concentrations of DX-52-1 (Figure 8B), which could be the result of some non-specific alkylation. These data suggest that the primary site of modification of radixin by DX-52-1 is not the site of phosphorylation by GRK2. Ultimately, this appears consistent with our previous result that DX-52-1 does not disrupt interactions with EBP-50 [9], since if DX-52-1 were blocking activating phosphorylation of ERM proteins, one would expect all interactions of activated ERM proteins to be affected.

We also found that both ezrin and moesin were labeled by biotinylated DX-52-1, though far less intensely than is radixin (Figure 8A). Compared to binding to radixin, binding was much weaker to ezrin and weaker still to moesin. These results suggest that biotinylated DX-52-1 binds ezrin and moesin far more slowly than it does radixin. The data are also consistent with our initial identification of radixin as the major binding protein for biotinylated DX-52-1 following unbiased, affinity-guided purification from MDCK cell extracts [9] and demonstrate that DX-52-1 exhibits considerable selectivity for radixin over the other ERM proteins.

Acknowledgments

We thank Christian Roy (Université de Montpellier, France) for the ezrin cDNA construct, Vijaya Ramesh (Massachusetts General Hospital) for the moesin construct, Philip Wedegaertner (Thomas Jefferson University) for the GRK2 and GRK2-K220R constructs, Richard A. Cerione (Cornell University) for the PAK3 PBD construct and Robert J. Lefkowitz (Duke University) for a sample of purified GRK2 protein. This work was supported by the National Institutes of Health (GM077622 to G.F.).

References

1. Fenteany G, Janmey PA, Stossel TP. Signaling pathways and cell mechanics involved in wound closure by epithelial cell sheets. Curr Biol 2000;10:831–838. [PubMed: 10899000]
2. Farooqui R, Fenteany G. Multiple rows of cells behind an epithelial wound edge extend cryptic lamellipodia to collectively drive cell-sheet movement. J Cell Sci 2005;118:51–63. [PubMed: 15585576]
3. Altan ZM, Fenteany G. c-Jun N-terminal kinase regulates lamellipodial protrusion and cell sheet migration during epithelial wound closure by a gene expression-independent mechanism. Biochem Biophys Res Commun 2004;322:56–67. [PubMed: 15313173]
4. Zhu S, Mc Henry KT, Lane WS, Fenteany G. A chemical inhibitor reveals the role of Raf kinase inhibitor protein in cell migration. Chem Biol 2005;12:981–991. [PubMed: 16183022]
5. Santy LC, Casanova JE. Activation of ARF6 by ARNO stimulates epithelial cell migration through downstream activation of both Rac1 and phospholipase D. J Cell Biol 2001;154:599–610. [PubMed: 11481345]
6. Farooqui R, Zhu S, Fenteany G. Glycogen synthase kinase-3 acts upstream of ADP-ribosylation factor 6 and Rac1 to regulate epithelial cell migration. Exp Cell Res 2006;312:1514–1525. [PubMed: 16529739]
7. Jaffe AB, Hall A. Rho GTPases: biochemistry and biology. Annu Rev Cell Dev Biol. 2005
8. Heasman SJ, Ridley AJ. Mammalian Rho GTPases: new insights into their functions from in vivo studies. Nat Rev Mol Cell Biol 2008;9:690–701. [PubMed: 18719708]
9. Kahsai AW, Zhu S, Wardrop DJ, Lane WS, Fenteany G. Quinocarmycin analog DX-52-1 inhibits cell migration and targets radixin, disrupting interactions of radixin with actin and CD44. Chem Biol 2006;13:973–983. [PubMed: 16984887]
10. Bretscher A, Chambers D, Nguyen R, Reczek D. ERM-Merlin and EBP50 protein families in plasma membrane organization and function. Annu Rev Cell Dev Biol 2000;16:113–143. [PubMed: 11031232]

NIH-PA Author Manuscript

NIH-PA Author Manuscript

NIH-PA Author Manuscript

11. Louvet-Vallee S. ERM proteins: from cellular architecture to cell signaling. Biol Cell 2000;92:305–316. [PubMed: 11071040]
12. Bretscher A, Edwards K, Fehon RG. ERM proteins and merlin: integrators at the cell cortex. Nat Rev Mol Cell Biol 2002;3:586–599. [PubMed: 12154370]
13. Hoeflich KP, Ikura M. Radixin: cytoskeletal adopter [*sic*] and signaling protein. Int J Biochem Cell Biol 2004;36:2131–2136. [PubMed: 15313460]
14. Fievet B, Louvard D, Arpin M. ERM proteins in epithelial cell organization and functions. Biochim Biophys Acta 2007;1773:653–660. [PubMed: 16904765]
15. Mc Clatchey AI, Fehon RG. Merlin and the ERM proteins--regulators of receptor distribution and signaling at the cell cortex. Trends Cell Biol 2009;19:198–206. [PubMed: 19345106]
16. Khanna C, Wan X, Bose S, Cassaday R, Olomu O, Mendoza A, Yeung C, Gorlick R, Hewitt SM, Helman LJ. The membrane-cytoskeleton linker ezrin is necessary for osteosarcoma metastasis. Nat Med 2004;10:182–186. [PubMed: 14704791]
17. Yu Y, Khan J, Khanna C, Helman L, Meltzer PS, Merlino G. Expression profiling identifies the cytoskeletal organizer ezrin and the developmental homeoprotein Six-1 as key metastatic regulators. Nat Med 2004;10:175–181. [PubMed: 14704789]
18. Wan X, Mendoza A, Khanna C, Helman LJ. Rapamycin inhibits ezrin-mediated metastatic behavior in a murine model of osteosarcoma. Cancer Res 2005;65:2406–2411. [PubMed: 15781656]
19. Kahsai AW, Cui J, Kaniskan HU, Garner PP, Fenteany G. Analogs of tetrahydroisoquinoline natural products that inhibit cell migration and target galectin-3 outside of its carbohydrate-binding site. J Biol Chem 2008;283:24534–24545. [PubMed: 18556657]
20. Matsui T, Maeda M, Doi Y, Yonemura S, Amano M, Kaibuchi K, Tsukita S. Rho-kinase phosphorylates COOH-terminal threonines of ezrin/radixin/moesin (ERM) proteins and regulates their head-to-tail association. J Cell Biol 1998;140:647–657. [PubMed: 9456324]
21. Oshiro N, Fukata Y, Kaibuchi K. Phosphorylation of moesin by Rho-associated kinase (Rho-kinase) plays a crucial role in the formation of microvilli-like structures. J Biol Chem 1998;273:34663–34666. [PubMed: 9856983]
22. Tran Quang C, Gautreau A, Arpin M, Treisman R. Ezrin function is required for ROCK-mediated fibroblast transformation by the Net and Dbl oncogenes. EMBO J 2000;19:4565–4576. [PubMed: 10970850]
23. Ng T, Parsons M, Hughes WE, Monypenny J, Zicha D, Gautreau A, Arpin M, Gschmeissner S, Verveer PJ, Bastiaens PI, Parker PJ. Ezrin is a downstream effector of trafficking PKC-integrin complexes involved in the control of cell motility. EMBO J 2001;20:2723–2741. [PubMed: 11387207]
24. Pietromonaco SF, Simons PC, Altman A, Elias L. Protein kinase C-θ phosphorylation of moesin in the actin-binding sequence. J Biol Chem 1998;273:7594–7603. [PubMed: 9516463]
25. Nakamura N, Oshiro N, Fukata Y, Amano M, Fukata M, Kuroda S, Matsuura Y, Leung T, Lim L, Kaibuchi K. Phosphorylation of ERM proteins at filopodia induced by Cdc42. Genes Cells 2000;5:571–581. [PubMed: 10947843]
26. Baumgartner M, Sillman AL, Blackwood EM, Srivastava J, Madson N, Schilling JW, Wright JH, Barber DL. The Nck-interacting kinase phosphorylates ERM proteins for formation of lamellipodium by growth factors. Proc Natl Acad Sci USA 2006;103:13391–13396. [PubMed: 16938849]
27. Cant SH, Pitcher JA. G protein-coupled receptor kinase 2-mediated phosphorylation of ezrin is required for G protein-coupled receptor-dependent reorganization of the actin cytoskeleton. Mol Biol Cell 2005;16:3088–3099. [PubMed: 15843435]
28. Penela P, Ribas C, Aymerich I, Eijkelkamp N, Barreiro O, Heijnen CJ, Kavelaars A, Sanchez-Madrid F, Mayor F Jr. G protein-coupled receptor kinase 2 positively regulates epithelial cell migration. EMBO J 2008;27:1206–1218. [PubMed: 18369319]
29. Vaiskunaite R, Adarichev V, Furthmayr H, Kozasa T, Gudkov A, Voyno-Yasenetskaya TA. Conformational activation of radixin by G13 protein α subunit. J Biol Chem 2000;275:26206–26212. [PubMed: 10816569]
30. Henry MD, Gonzalez Agosti C, Solomon F. Molecular dissection of radixin: distinct and interdependent functions of the amino- and carboxy-terminal domains. J Cell Biol 1995;129:1007–1022. [PubMed: 7744951]

NIH-PA Author Manuscript

NIH-PA Author Manuscript

NIH-PA Author Manuscript

31. Roy C, Martin M, Mangeat P. A dual involvement of the amino-terminal domain of ezrin in F- and G-actin binding. J Biol Chem 1997;272:20088–20095. [PubMed: 9242682]
32. Murthy A, Gonzalez-Agosti C, Cordero E, Pinney D, Candia C, Solomon F, Gusella J, Ramesh V. NHE-RF, a regulatory cofactor for Na^+-H^+ exchange, is a common interactor for merlin and ERM (MERM) proteins. J Biol Chem 1998;273:1273–1276. [PubMed: 9430655]
33. Carman CV, Parent JL, Day PW, Pronin AN, Sternweis PM, Wedegaertner PB, Gilman AG, Benovic JL, Kozasa T. Selective regulation of $G\alpha_{q/11}$ by an RGS domain in the G protein-coupled receptor kinase, GRK2. J Biol Chem 1999;274:34483–34492. [PubMed: 10567430]
34. Sterne-Marr R, Tesmer JJ, Day PW, Stracquatanio RP, Cilente JA, O'Connor KE, Pronin AN, Benovic JL, Wedegaertner PB. G protein-coupled receptor kinase 2/$G\alpha_{q/11}$ interaction. A novel surface on a regulator of G protein signaling homology domain for binding $G\alpha$ subunits. J Biol Chem 2003;278:6050–6058. [PubMed: 12427730]
35. Bagrodia S, Taylor SJ, Creasy CL, Chernoff J, Cerione RA. Identification of a mouse p21Cdc42/Rac activated kinase. J Biol Chem 1995;270:22731–22737. [PubMed: 7559398]
36. Mc Henry KT, Ankala SV, Ghosh AK, Fenteany G. A non-antibacterial oxazolidinone derivative that inhibits epithelial cell sheet migration. ChemBioChem 2002;3:1105–1111. [PubMed: 12404636]
37. Andreoli C, Martin M, Le Borgne R, Reggio H, Mangeat P. Ezrin has properties to self-associate at the plasma membrane. J Cell Sci 1994;107:2509–2521. [PubMed: 7844168]
38. Bagrodia S, Derijard B, Davis RJ, Cerione RA. Cdc42 and PAK-mediated signaling leads to Jun kinase and p38 mitogen-activated protein kinase activation. J Biol Chem 1995;270:27995–27998. [PubMed: 7499279]
39. Ishikawa H, Tamura A, Matsui T, Sasaki H, Hakoshima T, Tsukita S. Structural conversion between open and closed forms of radixin: low-angle shadowing electron microscopy. J Mol Biol 2001;310:973–978. [PubMed: 11502006]
40. Loebrich S, Bahring R, Katsuno T, Tsukita S, Kneussel M. Activated radixin is essential for GABAA receptor α5 subunit anchoring at the actin cytoskeleton. EMBO J 2006;25:987–999. [PubMed: 16467845]
41. Pujuguet P, Del Maestro L, Gautreau A, Louvard D, Arpin M. Ezrin regulates E-cadherin-dependent adherens junction assembly through Rac1 activation. Mol Biol Cell 2003;14:2181–2191. [PubMed: 12802084]
42. Liu G, Voyno-Yasenetskaya TA. Radixin stimulates Rac1 and Ca^{2+}/calmodulin-dependent kinase, CaMKII: cross-talk with $G\alpha$13 signaling. J Biol Chem 2005;280:39042–39049. [PubMed: 16186118]
43. Mammoto A, Takahashi K, Sasaki T, Takai Y. Stimulation of Rho GDI release by ERM proteins. Methods Enzymol 2000;325:91–101. [PubMed: 11036595]
44. Ivetic A, Ridley AJ. Ezrin/radixin/moesin proteins and Rho GTPase signalling in leucocytes. Immunology 2004;112:165–176. [PubMed: 15147559]
45. Takahashi K, Sasaki T, Mammoto A, Takaishi K, Kameyama T, Tsukita S, Takai Y. Direct interaction of the Rho GDP dissociation inhibitor with ezrin/radixin/moesin initiates the activation of the Rho small G protein. J Biol Chem 1997;272:23371–23375. [PubMed: 9287351]
46. Takaishi K, Sasaki T, Kameyama T, Tsukita S, Takai Y. Translocation of activated Rho from the cytoplasm to membrane ruffling area, cell-cell adhesion sites and cleavage furrows. Oncogene 1995;11:39–48. [PubMed: 7624130]
47. Hirao M, Sato N, Kondo T, Yonemura S, Monden M, Sasaki T, Takai Y, Tsukita S. Regulation mechanism of ERM (ezrin/radixin/moesin) protein/plasma membrane association: possible involvement of phosphatidylinositol turnover and Rho-dependent signaling pathway. J Cell Biol 1996;135:37–51. [PubMed: 8858161]
48. Bourguignon LY, Zhu H, Shao L, Chen YW. CD44 interaction with Tiam1 promotes Rac1 signaling and hyaluronic acid-mediated breast tumor cell migration. J Biol Chem 2000;275:1829–1838. [PubMed: 10636882]
49. Palczewski K. GTP-binding-protein-coupled receptor kinases - two mechanistic models. Eur J Biochem 1997;248:261–269. [PubMed: 9346277]
50. Aragay AM, Mellado M, Frade JM, Martin AM, Jimenez-Sainz MC, Martinez AC, Mayor F Jr. Monocyte chemoattractant protein-1-induced CCR2B receptor desensitization mediated by the G protein-coupled receptor kinase 2. Proc Natl Acad Sci USA 1998;95:2985–2990. [PubMed: 9501202]

NIH-PA Author Manuscript

NIH-PA Author Manuscript

NIH-PA Author Manuscript

51. Lefkowitz RJ, Shenoy SK. Transduction of receptor signals by β-arrestins. Science 2005;308:512–517. [PubMed: 15845844]
52. Pronin AN, Morris AJ, Surguchov A, Benovic JL. Synucleins are a novel class of substrates for G protein-coupled receptor kinases. J Biol Chem 2000;275:26515–26522. [PubMed: 10852916]
53. Ruiz-Gomez A, Humrich J, Murga C, Quitterer U, Lohse MJ, Mayor F Jr. Phosphorylation of phosducin and phosducin-like protein by G protein-coupled receptor kinase 2. J Biol Chem 2000;275:29724–29730. [PubMed: 10884381]
54. Freeman JL, Gonzalo P, Pitcher JA, Claing A, Lavergne JP, Reboud JP, Lefkowitz RJ. β_2-Adrenergic receptor stimulated, G protein-coupled receptor kinase 2 mediated, phosphorylation of ribosomal protein P2. Biochemistry 2002;41:12850–12857. [PubMed: 12379128]
55. Wan KF, Sambi BS, Frame M, Tate R, Pyne NJ. The inhibitory γ subunit of the type 6 retinal cyclic guanosine monophosphate phosphodiesterase is a novel intermediate regulating p42/p44 mitogen-activated protein kinase signaling in human embryonic kidney 293 cells. J Biol Chem 2001;276:37802–37808. [PubMed: 11502744]
56. Dinudom A, Fotia AB, Lefkowitz RJ, Young JA, Kumar S, Cook DI. The kinase Grk2 regulates Nedd4/Nedd4-2-dependent control of epithelial Na+ channels. Proc Natl Acad Sci USA 2004;101:11886–11890. [PubMed: 15284439]
57. Carman CV, Som T, Kim CM, Benovic JL. Binding and phosphorylation of tubulin by G protein-coupled receptor kinases. J Biol Chem 1998;273:20308–20316. [PubMed: 9685381]
58. Haga K, Ogawa H, Haga T, Murofushi H. GTP-binding-protein-coupled receptor kinase 2 (GRK2) binds and phosphorylates tubulin. Eur J Biochem 1998;255:363–368. [PubMed: 9716377]
59. Pitcher JA, Hall RA, Daaka Y, Zhang J, Ferguson SS, Hester S, Miller S, Caron MG, Lefkowitz RJ, Barak LS. The G protein-coupled receptor kinase 2 is a microtubule-associated protein kinase that phosphorylates tubulin. J Biol Chem 1998;273:12316–12324. [PubMed: 9575184]
60. Niggli V, Andreoli C, Roy C, Mangeat P. Identification of a phosphatidylinositol-4,5-bisphosphate-binding domain in the N-terminal region of ezrin. FEBS Lett 1995;376:172–176. [PubMed: 7498535]
61. Matsui T, Yonemura S, Tsukita S. Activation of ERM proteins in vivo by Rho involves phosphatidyl-inositol 4-phosphate 5-kinase and not ROCK kinases. Curr Biol 1999;9:1259–1262. [PubMed: 10556088]
62. Nakamura F, Huang L, Pestonjamasp K, Luna EJ, Furthmayr H. Regulation of F-actin binding to platelet moesin in vitro by both phosphorylation of threonine 558 and polyphosphatidylinositides. Mol Biol Cell 1999;10:2669–2685. [PubMed: 10436021]
63. DebBurman SK, Ptasienski J, Benovic JL, Hosey MM. G protein-coupled receptor kinase GRK2 is a phospholipid-dependent enzyme that can be conditionally activated by G protein $\beta\gamma$ subunits. J Biol Chem 1996;271:22552–22562. [PubMed: 8798423]
64. Kameyama K, Haga K, Haga T, Kontani K, Katada T, Fukada Y. Activation by G protein $\beta\gamma$ subunits of β-adrenergic and muscarinic receptor kinase. J Biol Chem 1993;268:7753–7758. [PubMed: 8463305]
65. Lodowski DT, Barnhill JF, Pyskadlo RM, Ghirlando R, Sterne-Marr R, Tesmer JJ. The role of G$\beta\gamma$ and domain interfaces in the activation of G protein-coupled receptor kinase 2. Biochemistry 2005;44:6958–6970. [PubMed: 15865441]

NIH-PA Author Manuscript

NIH-PA Author Manuscript

NIH-PA Author Manuscript

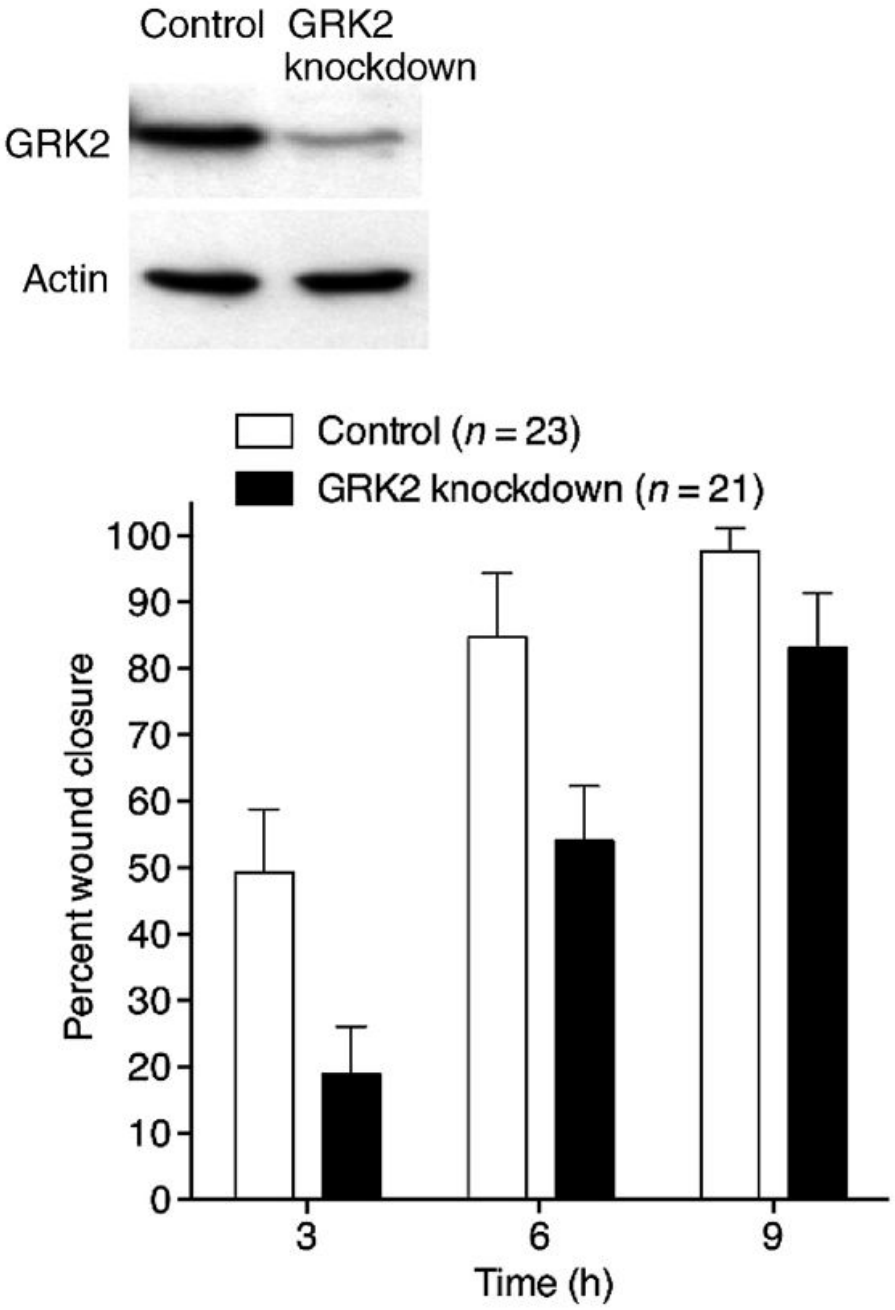

Figure 1. GRK2 positively regulates wound closure

RNA interference-based silencing of GRK2 expression delays wound closure in MDCK cell monolayers. Western blots of whole-cell lysates from control and stable GRK2-knockdown cells (GRK2 knockdown) probed with anti-GRK2 and anti-actin antibodies are shown above the bar graph, demonstrating knockdown of GRK2. Mean percent wound closure values with standard errors of the mean (SEM) are shown at three times post-wounding for the indicated number of wounds from three independent experiments is shown in the graph. The smaller difference between the values for control and GRK2-knockdown cells at 9 h is due to the fact that wounds in the control monolayers had largely closed already by 9 h for the size of wounds made in these experiments.

NIH-PA Author Manuscript

NIH-PA Author Manuscript

NIH-PA Author Manuscript

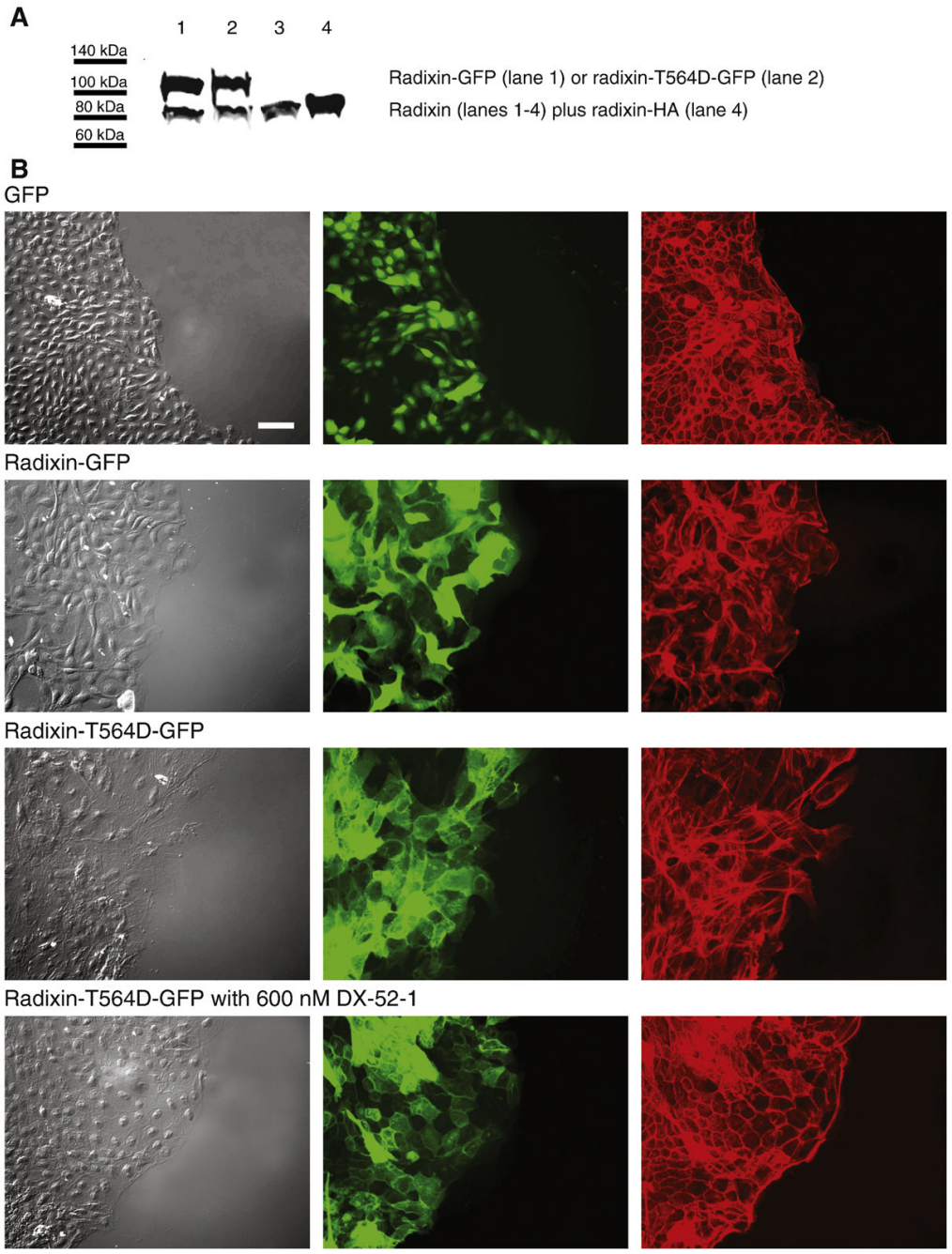

NIH-PA Author Manuscript
NIH-PA Author Manuscript
NIH-PA Author Manuscript

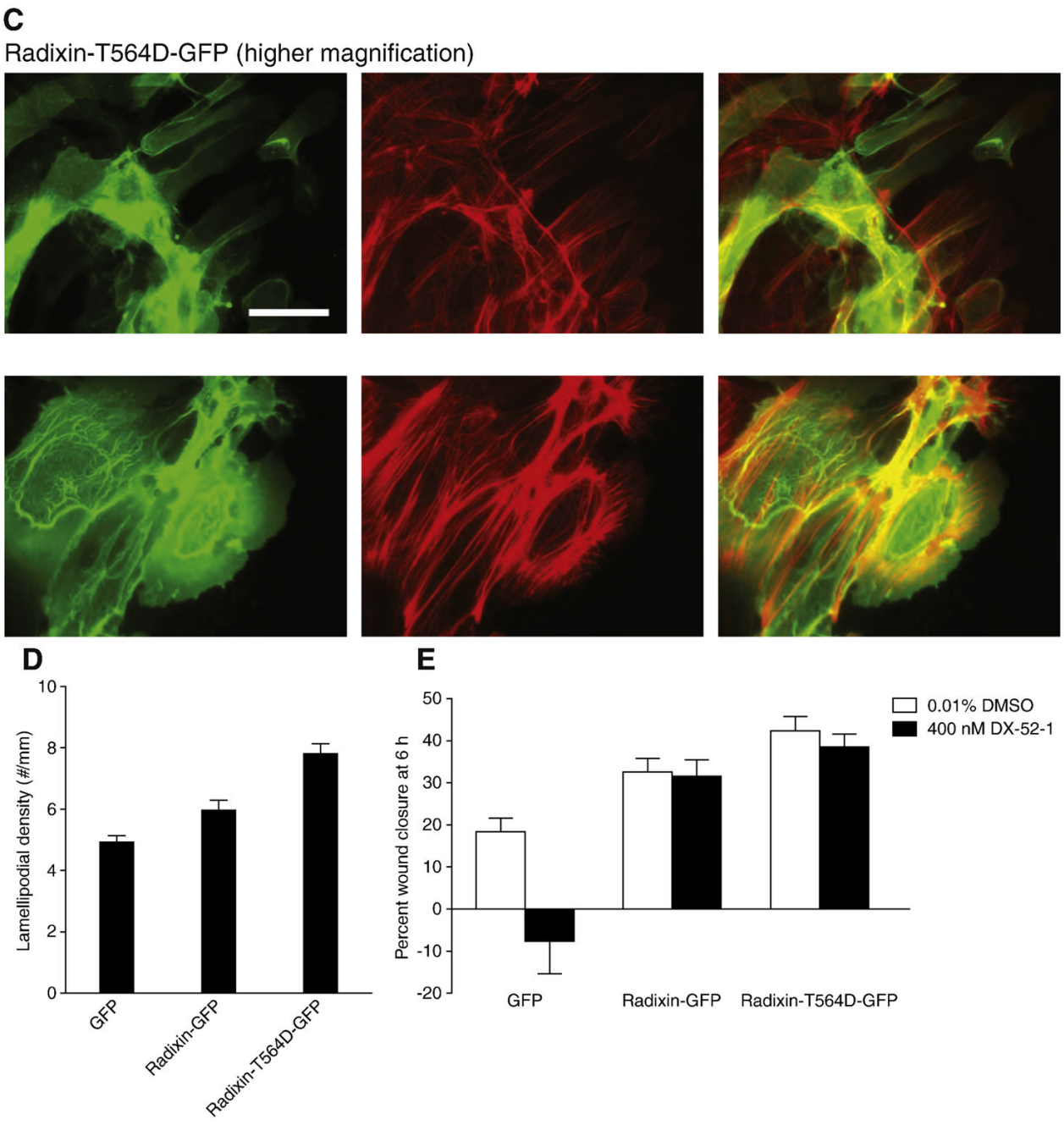

Figure 2. Expression of wild-type radixin and constitutively active radixin results in increased membrane protrusion and motility

(A) Representative Western blot of whole-cell lysates from MDCK cells stably expressing radixin-GFP (lane 1), constitutively active, phosphomimetic radixin-T564D-GFP mutant (lane 2) or radixin-HA (lane 4; the radixin-HA cells were used in the experiment described in Figure 7) probed with anti-radixin antibody. Lane 3 consists of non-transfected MDCK cells, showing expression of endogenous radixin alone. The levels of expression were calculated from the intensity of bands on three separate Western blots as 222% for radixin-GFP, 137% for radixin-T564D-GFP and 112% for radixin-HA that of endogenous radixin. (B) Fluorescence images of wounded monolayers of cells expressing GFP alone, radixin-GFP or radixin-T564D-GFP

NIH-PA Author Manuscript

NIH-PA Author Manuscript

NIH-PA Author Manuscript

in the presence or absence of the radixin inhibitor DX-52-1, as indicated. Confluent monolayers of MDCK cells stably expressing GFP alone, radixin-GFP or radixin-T564D-GFP were wounded and then fixed 6 h later and processed for imaging. From left to right, each row consists of a differential interference contrast image, a fluorescence image showing GFP fluorescence and a second fluorescence image showing TRITC-phalloidin staining of filamentous actin. All images in B are at the same magnification, with the scale bar corresponding to 50 μm. (C) Higher magnification fluorescence images of wounded sheets of cells expressing GFP alone or radixin-T564D-GFP 6 h after wounding. From left to right, each row consists of a fluorescence image showing GFP fluorescence, a second fluorescence image showing TRITC-phalloidin staining of filamentous actin and a merged image. All images in C are at the same magnification, with the scale bar corresponding to 50 μm. (D) Lamellipodial density at the wound margin (number of lamellipodial membrane protrusions at the wound edge divided by margin perimeter length) 6 h after wounding of monolayers of cells expressing GFP alone, radixin-GFP or radixin-T564D-GFP-expressing cells. Values are mean and SEM for 6 wounds from three independent experiments. (E) Percent wound closure at 6 h post-wounding in monolayers of cells expressing GFP alone, radixin-GFP and radixin-T564D-GFP in the presence or absence of DX-52-1 (mean and SEM for 12 wounds in each case from three independent experiments).

NIH-PA Author Manuscript
NIH-PA Author Manuscript
NIH-PA Author Manuscript

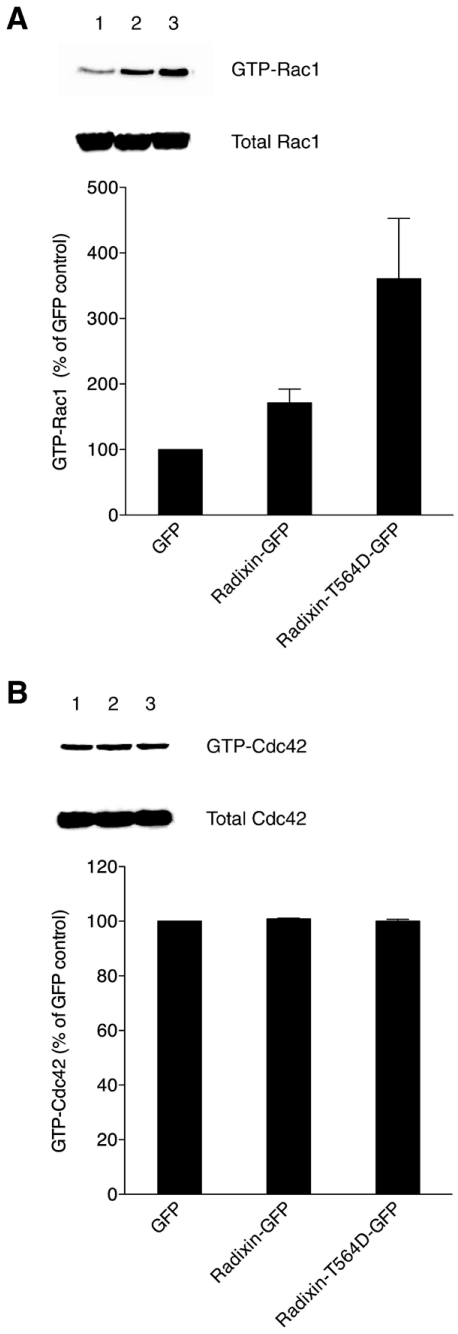

Figure 3. Rac1 activity is elevated in cells expressing constitutively active radixin

Pull-down of activated GTP-bound Rac1 (A) and GTP-bound Cdc42 (B) was performed from extracts prepared from MDCK cells expressing GFP alone (lane 1), radixin-GFP (lane 2) or radixin-T564D-GFP (lane 3). Representative Western blots for activated and total Rac1 and Cdc42 are shown, along with graphed data derived from quantitated band intensities for three independent experiments (mean and SEM), with values expressed as a percent of the levels of GTP-Rac1 or GTP-Cdc42 in control cells expressing GFP alone (normalization to the parallel control for each experiment prior to statistics).

NIH-PA Author Manuscript
NIH-PA Author Manuscript
NIH-PA Author Manuscript

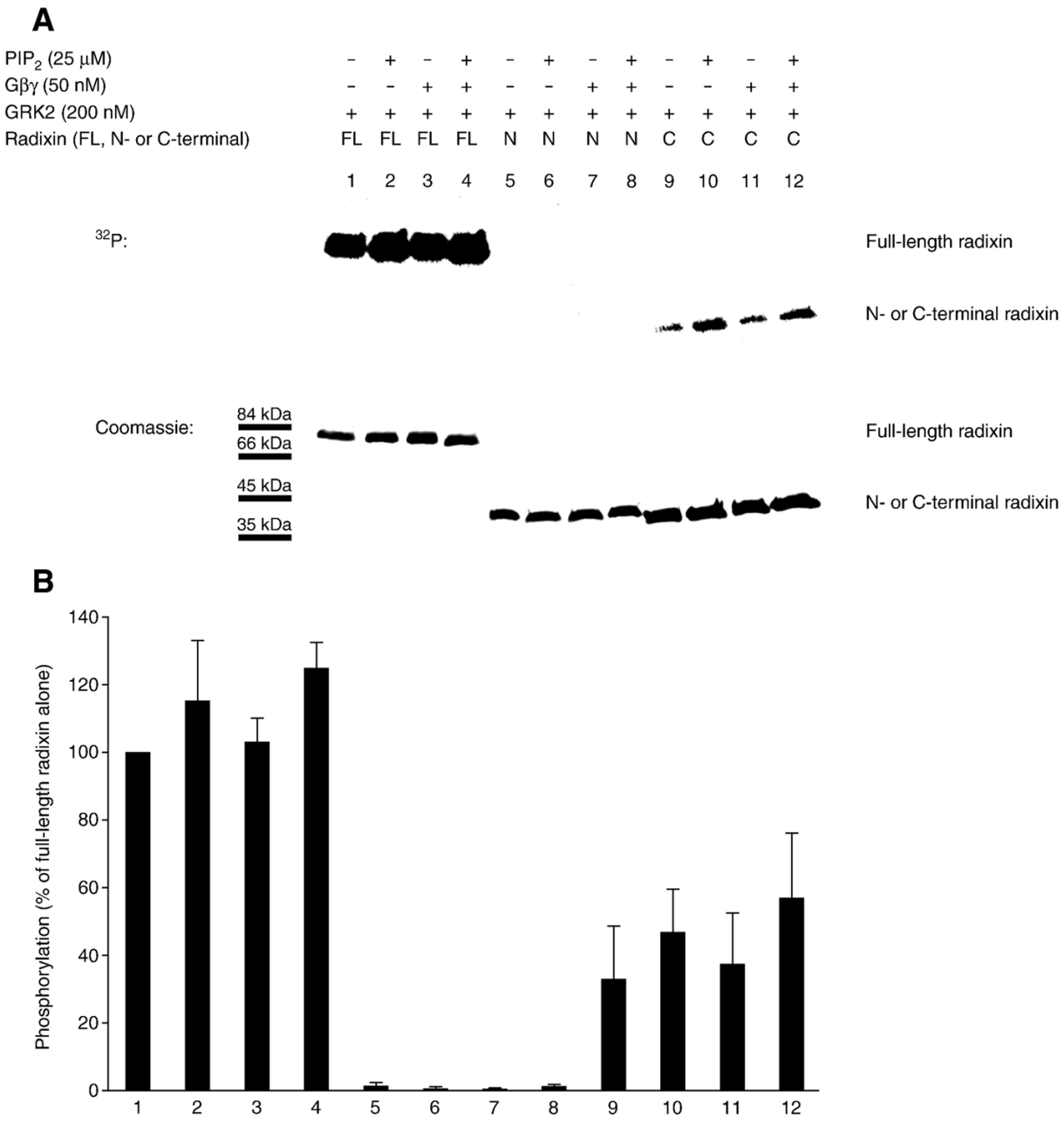

Figure 4. GRK2 phosphorylates the C-terminal region of radixin *in vitro*

(A) Kinase assays were performed with purified recombinant GRK2 and recombinant full-length radixin (FL; lanes 1, 2, 3 and 4), N-terminal radixin fragment (N-term; lanes 5, 6, 7 and 8) and C-terminal radixin fragment (C-term; lanes 9, 10, 11 and 12), in the absence (lanes 1, 5 and 9) or presence of PIP_2 (lanes 2, 4, 6, 8, 10 and 12) or Gβγ subunits (lanes 3, 4, 7, 8, 11 and 12). [γ-^{32}P]-ATP-labeled protein is shown in the autoradiogram at the top, while total Coomassie blue-stained protein is shown for equivalent loadings at the bottom. (B) Levels (mean and SEM) of [γ-^{32}P]-ATP-labeled protein quantitated from autoradiograms from four independent experiments as in A are shown, with values expressed as a percent of the level of phosphorylation of full-length radixin alone (without PIP_2 or Gβγ subunits) by GRK2 (normalization to the parallel full-length radixin result for each experiment prior to statistics).

NIH-PA Author Manuscript
NIH-PA Author Manuscript
NIH-PA Author Manuscript

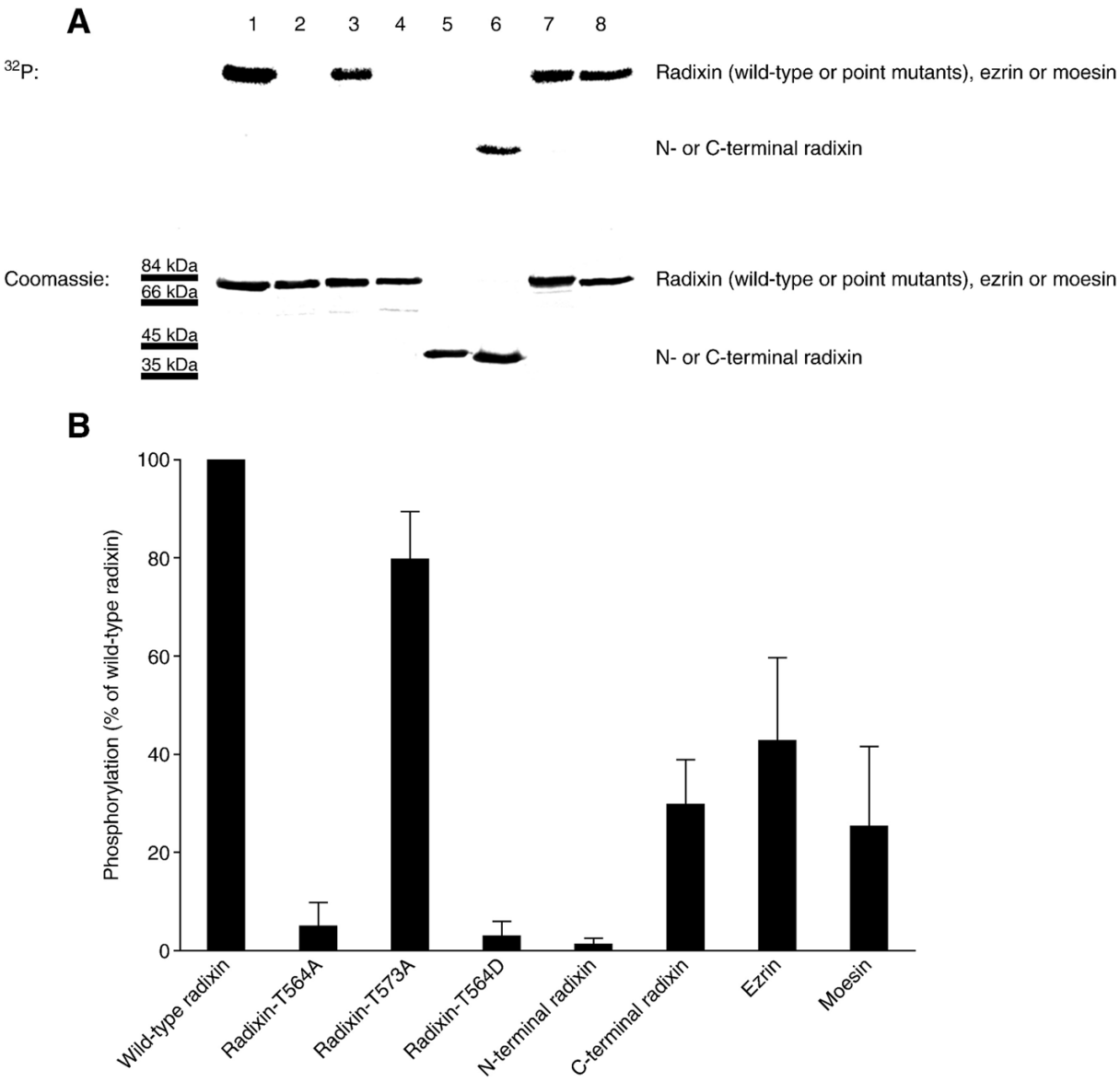

Figure 5. GRK2 phosphorylates radixin on Thr 564 *in vitro*

(A) Kinase assays were performed with purified recombinant GRK2 and wild-type radixin (lane 1), non-phosphorylatable radixin-T564A mutant (lane 2), non-phosphorylatable radixin-T573A mutant (lane 3), constitutively active, phosphomimetic radixin-T564D mutant (lane 4), N-terminal radixin fragment (lane 5), C-terminal radixin fragment (lane 6), ezrin (lane 7) and moesin (lane 8). [γ-^{32}P]-ATP-labeled protein is shown in the autoradiogram at the top, while total Coomassie blue-stained protein is shown for equivalent loadings at the bottom. (B) Levels (mean and SEM) of [γ-^{32}P]-ATP-labeled protein quantitated from autoradiograms from three independent experiments as in A are shown, with values expressed as a percent of the level of phosphorylation of full-length wild-type radixin by GRK2 (normalization to the parallel wild-type radixin result for each experiment prior to statistics).

NIH-PA Author Manuscript
NIH-PA Author Manuscript
NIH-PA Author Manuscript

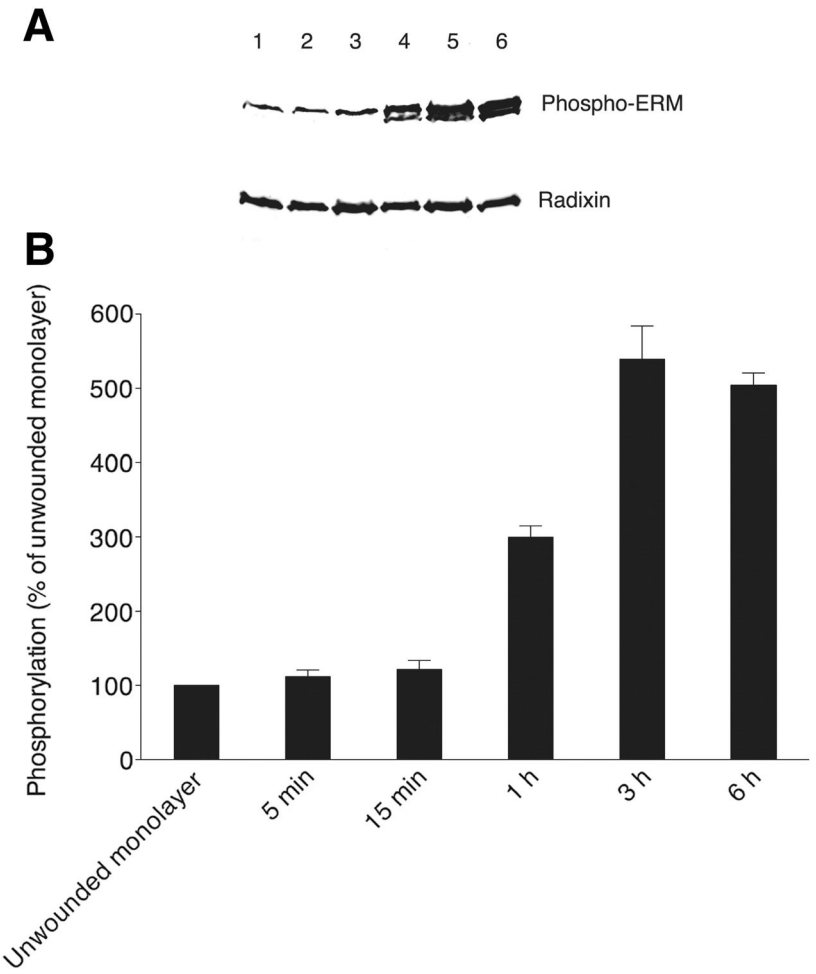

Figure 6. Phosphorylation of ERM proteins increases during the most active migratory phase of wound closure

(A) Phospho-ERM levels are shown on a representative Western blot probed with anti-phospho-ERM antibody at the top for an unwounded monolayer (lane 1) and at the following times after wounding: 5 min (lane 2), 15 min (lane 3), 1 h (lane 4), 3 h (lane 5) and 6 h (lane 6). The same blot stripped and reprobed with anti-radixin antibody is shown at the bottom. (B) Levels (mean and SEM) of ERM phosphorylation as a function of time after wounding are shown, derived from band intensities on Western blots for three separate experiments as in A, with values expressed as a percent of the level of phospho-ERM in unwounded monolayers (normalization to the parallel unwounded monolayer for each experiment prior to statistics).

NIH-PA Author Manuscript
NIH-PA Author Manuscript
NIH-PA Author Manuscript

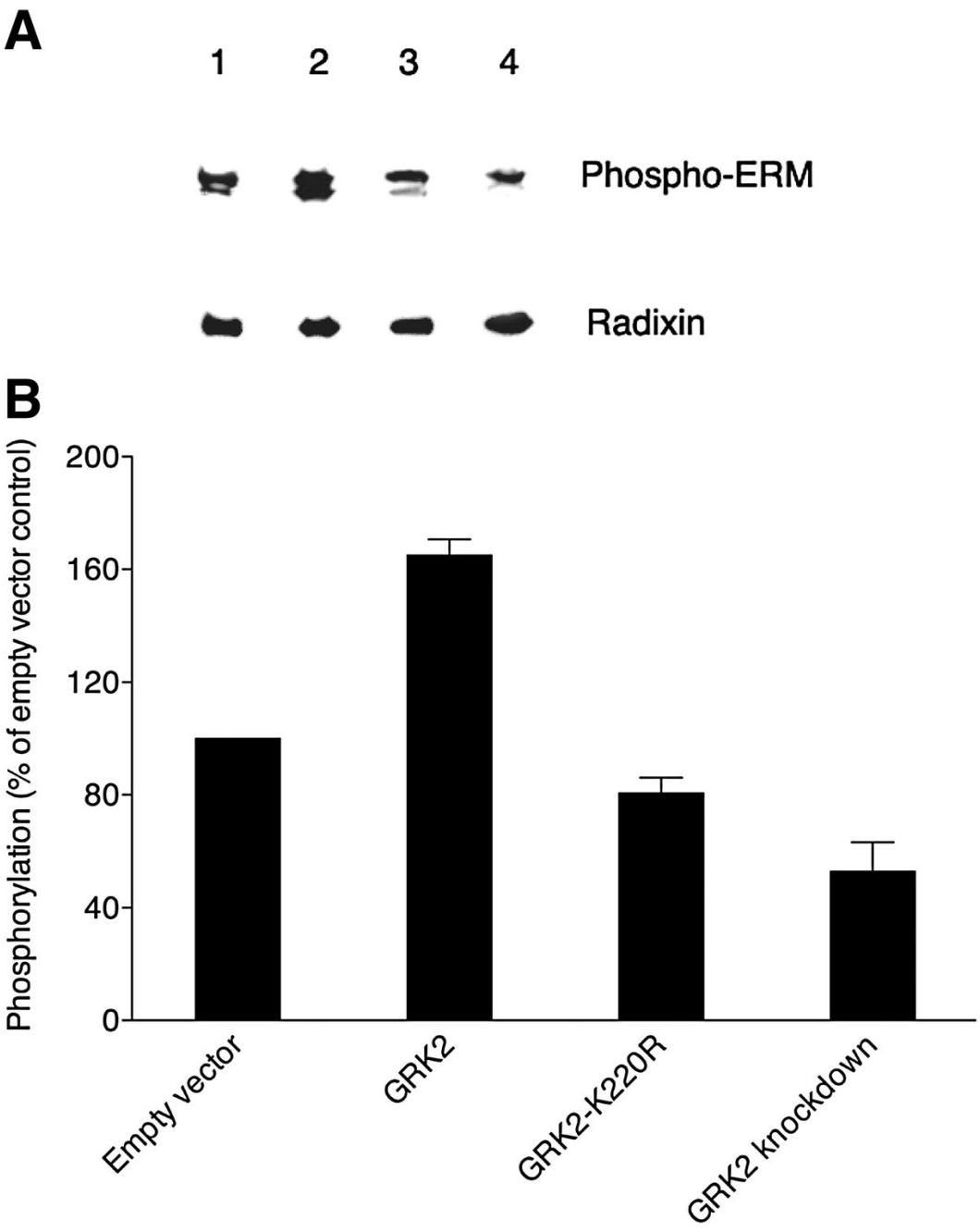

Figure 7. GRK2-dependent phosphorylation of ERM proteins in MDCK cells

(A) A representative Western blot probed with phospho-ERM antibody is shown at the top for extracts from confluent MDCK cell cultures stably expressing radixin-HA that were then transiently transfected with empty vector (lane 1), wild-type GRK2 (lane 2), kinase-dead GRK2-K220R mutant (lane 3) or GRK2-specific shRNA (GRK2 knockdown; lane 4). The same blot stripped and reprobed with anti-radixin antibody is shown at the bottom. (B) Levels (mean and SEM) of phosphorylated ERM proteins are shown, derived from band intensities on Western blots for three separate experiments as in A and expressed as a percent of the level for empty vector controls (normalization to the parallel control for each experiment prior to statistics).

NIH-PA Author Manuscript
NIH-PA Author Manuscript
NIH-PA Author Manuscript

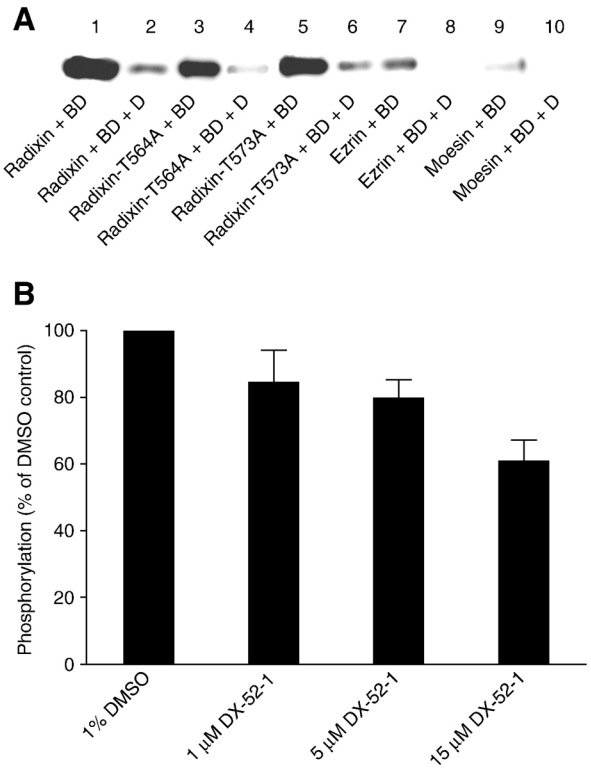

Figure 8. Thr 564 and Thr 573 are not the sites of modification by DX-52-1 on radixin, and ezrin and moesin are also modified by DX-52-1, but much less intensely than radixin

(A) DX-52-1 binds the Thr-to-Ala radixin mutants (radixin-T564A and radixin-T573A), along with wild-type radixin, but only very weakly binds ezrin and moesin. DX-52-1-binding experiments were performed as described in Materials and Methods with 23 μM of each purified recombinant protein and 10 μM biotinylated DX-52-1 with or without 500 μM of free, unlabeled DX-52-1 (added simultaneously as competitor to verify saturability and specificity). Proteins and treatments are: wild-type radixin, biotinylated DX-52-1 (lane 1); wild-type radixin, biotinylated DX-52-1 (BD) with 50× free, unlabeled DX-52-1 (D; lane 2); radixin-T564A, biotinylated DX-52-1 (lane 3); radixin-T564A, biotinylated DX-52-1 with 50× DX-52-1 (lane 4); radixin-T573A, biotinylated DX-52-1 (lane 5); radixin-T573A, biotinylated DX-52-1 with 50× DX-52-1 (lane 6); ezrin, biotinylated DX-52-1 (lane 7); ezrin, DX-52-1 with 50× DX-52-1 (lane 8); moesin, biotinylated DX-52-1 (lane 9); moesin, biotinylated DX-52-1 with 50× DX-52-1 (lane 10). (B) DX-52-1 does not block phosphorylation of radixin by GRK2. Purified recombinant GRK2 was preincubated with different concentrations of DX-52-1, followed by assay of kinase activity toward radixin, as described in Materials and Methods. Levels (mean and SEM) of [γ-^{32}P]-ATP-labeled radixin were quantitated from autoradiograms from three independent experiments, with values expressed as a percent of the level of the phosphorylated radixin signal for DMSO controls (normalization to the parallel control for each experiment prior to statistics).